Journal of Materials Chemistry C

Accepted Manuscript

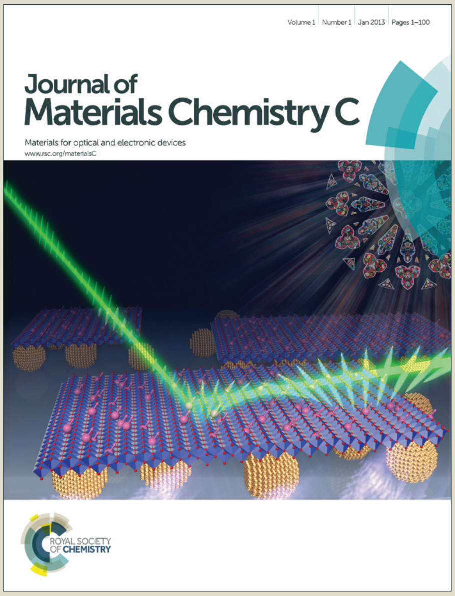

ROYAL SOCIETY OF CHEMISTRY

www.rsc.org/materialsC

Journal Name

RSCPublishing

ARTICLE

Cite this: DOI: 10.1039/x0xx00000x

Received 00th January 2012,
Accepted 00th January 2012

DOI: 10.1039/x0xx00000x

www.rsc.org/

Characterization of precursor-based ZnO transport layers in inverted polymer solar cells

Nadia Grossiord [a,*], Paul de Bruyn, [b,c] Date J. D. Moet, [a] Ronn Andriessen, [a] Paul W. M. Blom [d,e]

A wide range of characterization techniques are used to study spin-coated films of zinc oxide (ZnO) obtained from thermal decomposition of zinc acetylacetonate hydrate. Inverted organic solar cells with ZnO transport layers were prepared. Deposition conditions of the solution onto the substrate (e.g. substrate temperature) were found to be crucial in order to obtain well-performing inverted cells. Interestingly, it is demonstrated that full conversion of the precursor into crystalline ZnO is not necessary to prepare well-operating cells.

Introduction

Over the last years, increasing efforts were devoted to the research and development of organic electronics produced on flexible substrates. Semiconducting polymers are very promising materials as they are soluble in many organic solvents, allowing deposition by solution printing or coating. The prospect to produce large amounts of light-weight, flexible organic photovoltaic devices by roll-to-roll (R2R) processing makes this technology very attractive as it would render the production of this type of cells economically competitive. Additionally, the technology should allow for the production of flexible and (semi-)transparent organic photovoltaic (OPV) modules with a large freedom of design, opening ways to new applications such as portable charging of small devices which could, for example, be integrated in clothing and bags.[1-5]

However to achieve low costs all material layers in the device, including the injecting contacts, should be deposited from solution to fully benefit from a cheap production method such as R2R processing. In practice this excludes the use of low work function metal cathodes, since they generally have to be evaporated in vacuum and are extremely sensitive to oxygen and moisture. Among the materials used as cathode or electron transport layer, *n*-type metal oxides have received considerable attention due to their enhanced ambient stability over low work function metals and n-type doped organic materials. Furthermore, their high optical transparency makes them suited as low work function cathodes[6-8] in inverted solar cells and as recombination layers in tandem solar cells.[9,10] In particular zinc oxide (ZnO) is a promising material due to its environmental stability, high transparency and compatibility with various deposition techniques. Two main strategies to prepare ZnO buffer layers from solution were explored over the past years:

(i) synthesis of ZnO nanoparticles followed by a dispersion in a given solvent to obtain a colloidal suspension of nanoparticles, which can be processed by different methods such as spin coating or slot die coating at room temperature, preferably without any (thermal) post-deposition treatment, [6,11]

(ii) dissolution of a precursor in a solvent which is deposited on a substrate by spin coating or printing; [12,13] the conversion from the precursor to ZnO occurs after deposition onto the substrate.

In the first case, the nanoparticle characteristics and properties are mainly determined by the synthesis parameters and are not expected to be dramatically modified by the deposition step, which can typically be performed at room temperature. Nevertheless, per definition, colloidal suspensions made of nanoparticles dispersed in a solvent system are metastable. As a result, they may undergo aggregation upon storage due to, for example, temperature changes, which is undesirable for printing purposes. Additionally, modifying the dispersing medium can significantly alter the aggregation state of the nanoparticles.[6] Another drawback highlighted by Krebs and coworkers [6,11] while using this type of nanoparticle dispersions to prepare inverted OPV cells in air is that they are sensitive to humidity and need therefore to be stabilized with e.g. methoxyethoxyacetic acid (MEA). Addition of the latter slows down the drying of the deposited layer, which can last several hours at 140 °C. Moreover, in order to prevent the nanoparticles from dissolving in the subsequently processed layer, cross-linking agents must be added, requiring longer drying time and/or higher temperatures which are not always compatible with R2R processing on a flexible plastic substrate.

An alternative to the synthesis of nanoparticles is the precursor approach. However, here the properties of the final ZnO layer are strongly dependent on sample history and method of preparation. In other words, adjusting processing and post-deposition parameters (e.g. temperature) is crucial in order to tune ZnO layer properties and hence the final performance of the OPV device. Reports dealing with the use of e.g. cation hydration chemistry or of the decomposition of molecular zinc complex as single source precursor to obtain thin ZnO layers [12,13] use relatively high post-deposition temperatures (150 °C and above) and/or long process times (of the order of minutes, if not hour).

Recently, solar cells with a precursor-based zinc oxide transport layer and low reflective light absorber on glass were reported.[7] Zinc acetylacetonate hydrate ($Zn(acac)_2 . H_2O$) dissolved in ethanol was spin coated on glass/ITO and annealed at 120 ºC for 30 s. The performance of solar cells with an inverted structure, namely ITO/ZnO/photoactive layer (PAL)/MoO_3/Al, was shown to be equivalent to the ones of conventional cells with a bottom anode-top cathode configuration for various conjugated polymers.

For R2R produced devices manufactured on plastic substrates such as polyethylene terephthalate (PET) or polyethylene naphthalate (PEN), low-temperature deposition of metal oxide layers is highly desirable.

To become economically competitive, R2R heating steps, such as the one required for $Zn(acac)_2$ annealing, should be kept as short as possible in order to minimize the length of the drying unit. Moreover, in order to prevent any significant damage of the plastic substrate, annealing temperatures should not exceed 130 °C.

To elucidate which requirements the solution-processed ZnO electron transport layer (ETL) from a precursor must fulfill as part of well performing organic solar cells, a systematic study is warranted. In this article, we report on the characterization of zinc acetylacetonate-based zinc oxide layers. A broad range of techniques such as focused-ion beam scanning electron microscopy (FIB-SEM), X-Ray diffraction (XRD) and X-Ray reflectivity (XRR), thermogravimetric analysis (TGA), modulated differential scanning calorimetry (MDSC), Fourier-transform infrared (FTIR) spectroscopy and atomic force microscopy (AFM) are used to characterize the exact nature of the layer before and after precursor conversion. Additionally, inverted solar cells were prepared where the ZnO layer deposition was systematically varied in order to determine a suitable processing window.

Experimental section

Sample preparation

Zinc acetylacetonate hydrate ($C_{10}H_{14}O_4Zn{\cdot}H_2O$ or $Zn(acac)_2\ {\cdot}H_2O$) was purchased from Sigma-Aldrich (99.995 % purity) and used as received. Solutions of 20 mg/mL in ethanol were prepared by dissolving the precursor at 50 ºC under stirring for several hours. The solution was subsequently filtered with a 0.45 µm PTFE filter. The precursor solution was very stable and could be stored for months at room temperature, without presenting any turbidity or white precipitate. Clean glass substrates sonicated in acetone and isopropanol were used as substrates. $Zn(acac)_2$ – ethanol solutions were spin coated on the glass substrates which had undergone an UV-ozone treatment in order to improve the wetting on the substrate during spin coating. Non pre-heated substrates kept at room temperature were used as such and spin-coated by the precursor solution hold at 50 °C. Pre-heated substrates were heated onto a hotplate and quickly transferred to the spin coater where they were immediately spin coated with the precursor solution also hold at 50 °C.

Solar cells were prepared by cleaning ITO coated glass substrates with a non-ionogenic detergent, before sonication in acetone and 2-propanol. Substrates were dried in an oven and cleaned by UV-ozone before spin casting procedures. PEDOT:PSS (Clevios P VP Al 4083) was spin cast under ambient conditions to yield a 50 nm thick layer. $Zn(acac)_2$ solutions from ethanol were spin coated at 50 °C and subsequently annealed at 120 °C in air on a hot plate. P3HT:PCBM blends (1:0.8 by weight; 15 mg/mL of polymer dissolved in chloroform) were spin cast in a nitrogen-filled glovebox. The solar cells were finished off with either a 1 nm LiF/100 nm Al cathode or a 10 nm MoO_3/100 nm Au anode, thermally evaporated under vacuum at a pressure lower than 10^{-6} mbar.

Measurements

A Leica **optical microscope** with EC3 camera was used to characterize the samples.

FIB-SEM: *Sample preparation*: The $Zn(acac)_2$-ethanol solution was spin-coated on glass substrates and subsequently annealed for 20 s at 120 ºC. Afterwards, the samples were coated in a sputter coater with a few-nm thick Pt layer to avoid charging. Subsequently a 1.0 µm Pt layer (electron- and ion-beam) is deposited in the FIB at the region of interest to protect the top layers during FIB milling. Milling was subsequently done with a Ga+ ion gun to open a trench in the sample. The electron gun for SEM is at a 42 º angle to the FIB column. As a result, it was possible to study cross-sections of the studied layers by tilting the sample. The study was done with a Philips Nova 200 Nanolab SDB (Small Dual Beam) using an acceleration voltage of 25 kV.

XRD and XRR: The $Zn(acac)_2$ – ethanol solution was spin coated on a glass plate in the same conditions as those used to prepare solar cells. The spin coated layers were subsequently annealed at 120 °C or 250 °C for various times. The samples were subsequently characterized with a PANalytical X'Pert PRO MPD diffractometer equipped with a Cu X-ray source and X'Celerator detector. Due to the low thickness of the samples studied, grazing incidence (GI) measurements were performed. The incident angle was fixed at 0.23° for the sample annealed for 20 s and at 0.24° for the one annealed for 4 hours. The step size for both measurements was 0.04°. The wavelength was 0.15406 nm (Cu Ka1 radiation). A parallel plate collimator with a 0.27° opening angle and a flat graphite monochromator were used in the diffracted beam. XRR measurements were performed to determine the ZnO layer thickness.

Surface topography measurements: AFM images were taken on a MultiMode AFM with a Nano-Scope IV Scanning Probe

Microscope Controller, mounting Si cantilevers and operated in tapping mode.

The **modulated differential scanning calorimetry** (**MDSC**) measurements were performed using a TA instruments Q 2000 DSC and Tzero, low mass aluminum sample pans.

The **thermo gravimetric analysis** (**TGA**) were performed using a TA instruments Q5000IR TGA and aluminum sample pans suspended in stainless steel bails.

J-V measurements of the solar cells were performed with a computer controlled Keithley 2400 SourceMeter. Quantum efficiency was measured with a setup built in-house.

In-situ FTIR: measurements were performed using a Thermo Nexus FTIR bench equipped with a heatable Golden Gate ATR Module. Samples made of thin films of Zn(acac)$_2$-ethanol solution spin coated on gold-coated silicon substrates were brought into contact with the Golden Gate ATR Module.

- For measurements of samples annealed at different temperatures, namely 120 and 200 °C, sample layers were spin coated and annealed for different times following the procedure detailed in the sample preparation section. These samples were then directly characterized by FTIR.
- For time-dependent measurements, Zn(acac)$_2$ layers were spin coated, without undergoing annealing. The temperature of the Golden Gate ATR Module was initially set at 40°C. Directly after a given sample was brought into contact with the module, the temperature of the latter was increased to 120 °C and FTIR spectra were recorded every 1.2 s for 20 minutes.

Results and discussion

Influence of the layer morphology

Since the ETL layer studied here comes from the thermal decomposition of a precursor, which leads to the formation of a metal oxide, it is apparent that the *post*-deposition parameters (e.g. annealing temperature, residual humidity of the atmosphere) strongly influence the composition of the layer. Less obvious is the influence of the deposition parameters themselves. It appears that the temperature of deposition of the Zn(acac)$_2$ – ethanol solution is crucial as the base morphology is strongly influenced by the processing.

Layers prepared by spin coating of Zn(acac)$_2$-ethanol on glass substrates maintained either at room temperature or heated at 50 °C were characterized by optical microscopy, see **Figure 1**. When the sample was spin coated in air with a solution maintained at room temperature or heated at 50ºC on a non-heated glass substrate, “needle-like” crystallized features were visible, see **Figure 1a**. It is worth noting that these features were observed before thermal annealing of the Zn(acac)$_2$ layer and remained unchanged after thermal treatment. In other words, the presence of these features is not related to the precursor decomposition and ZnO formation, but is rather linked to the Zn(acac)$_2$ properties. On the contrary, when the deposition was done on a pre-heated substrate (**Figure 1b**), the optical microscope analysis did not reveal the presence of any needle features. Most probably, in the second case, the elevated temperature of the substrate during deposition promotes rapid solvent evaporation before supersaturation of the Zn(acac)$_2$-ethanol solution and therefore hinders Zn(acac)$_2$ crystallization.

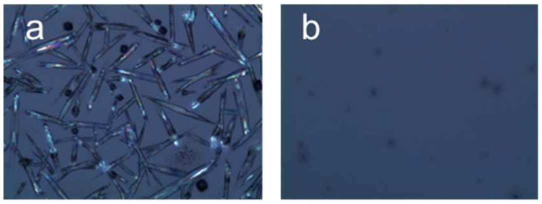

Fig. 1. Optical microscope pictures of Zn(acac)$_2$ layers spin coated from an ethanol solution on: (a) a non-heated substrate and (b) a substrate heated at 50 °C. Picture size: 31.1 × 98.3 μm^2.

FIB-SEM analysis gives more insight regarding the structure of these two types of layers. **Figure 2** displays pictures of the cross-sections of a layer prepared on a non-heated substrate (corresponding to **Figure 1a**). These layers were very rough and irregular; some of the needle features were as high as 140 nm (see **Figure 2c**). Locally the substrate was not even covered, resulting in the presence of holes in the layer.

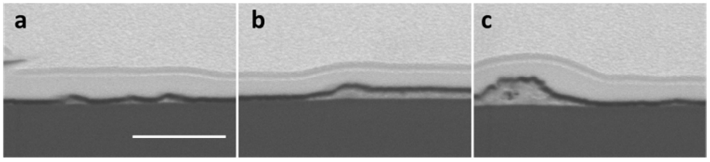

Fig. 2 a-c. FIB-SEM pictures of the cross-section of a Zn(acac)$_2$ layer spin-coated on a non-heated substrate and subsequently annealed at 120 °C for 20 s. The dark grey area underneath corresponds to the substrate, while the irregular layer deposited on top of it is the Zn(acac)$_2$ layer. The light grey layer covering the Zn(acac)$_2$ layer is the Pt layer needed for the FIB-SEM sample preparation. Scale bar: 400 nm.

On the contrary, layers resulting from the spin coating of Zn(acac)$_2$-ethanol solution on heated substrates appeared to be closed and smooth with homogeneous thickness over the whole coated area, see **Figure 3** (several locations checked).

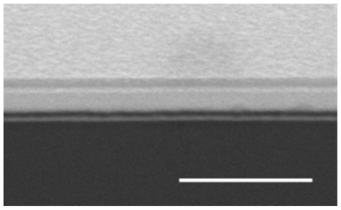

Fig. 3. FIB-SEM picture of a cross-section of a Zn(acac)$_2$ layer spin coated on a pre-heated substrate and subsequently annealed at 120

°C for 20 s. For description of the different layers, see caption of Figure 2. Scale bar: 400 nm.

To evaluate the surface roughness of the closed layer, AFM measurements were performed. **Figure 4** shows a view from the top of a flat layer sample surface (x- and y-axis) and the surface layer roughness (z-axis). The root mean squared (RMS) roughness of the layer, as determined from these images amounts to 1.7 nm.

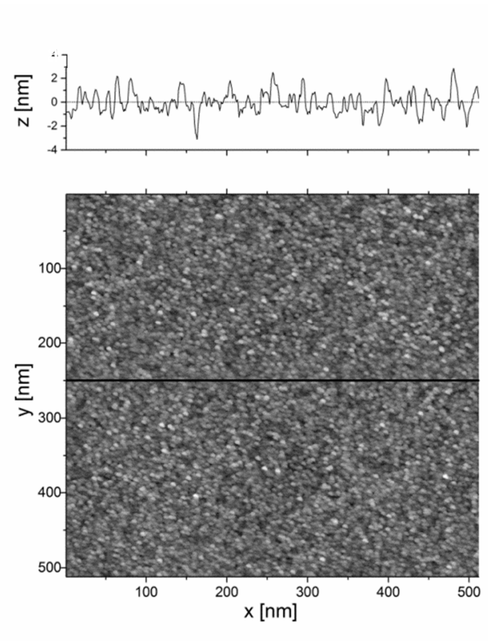

Fig. 4. AFM picture of a smooth ZnO layer with the roughness profile of the surface (z direction) at the location highlighted by the horizontal black line. Unit of the axis scale: nm.

Investigation of the chemical composition of the layer

Upon heating, zinc acetylacetonate decomposes to form zinc oxide.[14,15] This decomposition reaction has been studied in depth by Arii and Kishi.[16] Here, we aim to gain more insight regarding the decomposition of $Zn(acac)_2$ for use in electron transport layers for inverted organic solar cells.[7]

The decomposition of zinc acetylacetonate monohydrate ($Zn(acac)_2 \cdot H_2O$) was monitored by TGA under controlled atmosphere. The typical TGA curve for the precursor decomposition in dry nitrogen and in air is shown in **Figure 5.** Superimposition of MSDS and TGA graphs of the same sample showed that the precursor undergoes four endothermic transitions at comparable temperatures as the ones reported in Ref. 16. Mass losses occur in two main steps: one around 80-100 °C, and a second one from about 100 °C to 180 °C. At the end of the heating step, a small amount of residue remains in the crucible.

According to Arii and Kishi,[16] the precursor undergoes the following decomposition reaction:

$$Zn(CH_3COCHCOCH_3)_2.\ H_2O \rightarrow 2\ CH_3COCH_2COCH_3 + ZnO \qquad \text{Eq.1}$$

The first endothermic transition occurs between 80 and 100 °C. It is accompanied by a mass loss of 6.5 %, which is due to dehydration as it corresponds to the theoretical, calculated mass loss expected from thermal dehydration After this first transition, upon heating, the mass loss occurred in three successive steps which could clearly be evidenced with the differential gravimetric (DTG) thermograph. The three other endothermic transitions observed at temperatures higher than 100 °C were identified as the sum of sequential and parallel reactions including phase transition, fusion, evaporation and decomposition of $Zn(acac)_2$.[16] An important finding of the work of Arii and Kishi is that ZnO formation from $Zn(acac)_2$ occurs via the formation of an intermediate compound in dry nitrogen. The exact nature of this compound was not clearly identified.

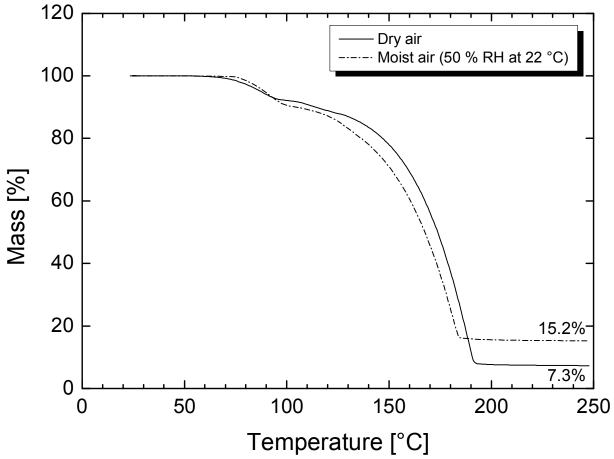

Fig. 5. TGA results of $Zn(acac)_2$ in dry and moist air (relative humidity of 50 %) for a heating rate of 10 °C/min.

After heating in dry nitrogen, the weight percentage of the remaining residue made of ZnO equals 7.3 % at 200 ºC, which is only 24 % of what could theoretically have been formed. This result indicates that sublimation of the precursor occurs during the heating of the sample. When the precursor decomposition was carried out in wet nitrogen with 50 % relative humidity (i.e. the level of humidity maintained in our clean room), the ZnO formation, thus the reaction yield, was increased significantly from 7.3 % to 15.2 % of the sample initial weight. These results were in line with the findings of Arii and Kishi and correspond to the lowest absolute humidity level examined.[16] They found that water vapor introduced in the atmosphere could prevent $Zn(acac)_2$ sublimation during heating and therefore lead to enhanced ZnO formation.

The earlier reported inverted cells on glass using a $Zn(acac)_2$-based ETL were annealed at only 120 °C,[7] suggesting that the precursor decomposition process was not complete. Nevertheless, it was found by Arii and Kishi that moisture present in the atmosphere plays the role of catalyst during the reaction of decomposition of the precursor, promoting the formation of ZnO even at relatively low temperatures. To confirm this, XRD measurements were performed on $Zn(acac)_2$ layers prepared in the same conditions as the ETL used in the inverted cells. The precursor solution was spin coated on two heated glass substrates. The resulting layer was subsequently annealed at 120 °C for 30 s and 4 hours. The results of these measurements are presented in **Figure 6**. The broad peak present at 20 º comes from the glass substrate. It can be seen that, even after 30 s annealing at 120 ºC, crystallization peaks corresponding to crystalline ZnO can be evidenced. The peaks are rather broad, most probably due to a small crystallite size. The difference of intensity of the signal at 35 º might indicate a difference in crystallite orientation. Extended annealing at 120 °C did not significantly increase the degree of crystallinity of the layer.

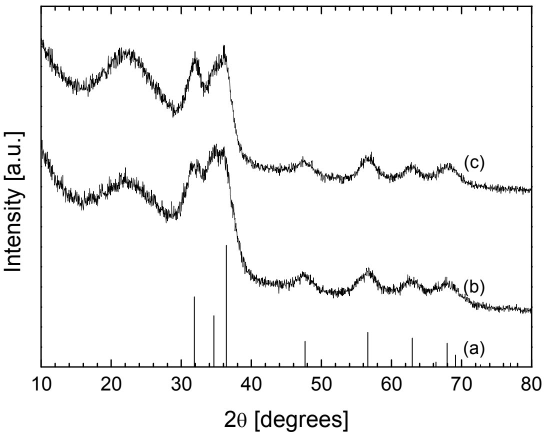

Fig. 6. Standard XRD pattern of ZnO **(a)** and grazing incidence diffractograms of the spin coated ZnO layers after annealing at 120 °C for 30 s **(b)** or 4 h **(c).**

XRR measurements indicated the presence of a layer possessing a density much lower than that of bulk ZnO (< 3 g/cm^3) [17] and a thickness of about 26 nm, which is of the same order of magnitude as the layer thickness measured by FIB-SEM, see **Figure 3**.

Interestingly, samples annealed for 30 s or 4 hours at a temperature at which full Zn(acac)$_2$ conversion is expected, i.e. 250 °C, based on TGA analysis (**Figure 5**), did not display a significantly higher degree of crystallinity than the samples annealed at 120 °C.

To get more insight in the chemical composition of the ETLs, FTIR measurements were performed on layers spin coated on gold-coated silicon substrates. The first spectrum taken before annealing of the layer was characteristic of Zn(acac)$_2$, see **Figures 7a**. After the sample was heated at 200 °C for 20 s, nearly complete conversion of Zn(acac)$_2$ could be observed since the two bands in the 1300-1800 cm^{-1} wavelength range were no longer visible (**Figure 7c)**. On the contrary, spectra recorded after 30 s of heating at 120 °C showed a significant, though incomplete, conversion of the precursor, see **Figure 7b**. This evidences that the Zn(acac)$_2$ thermal decomposition takes place within seconds in the experimental conditions used to prepare inverted OPV cells.

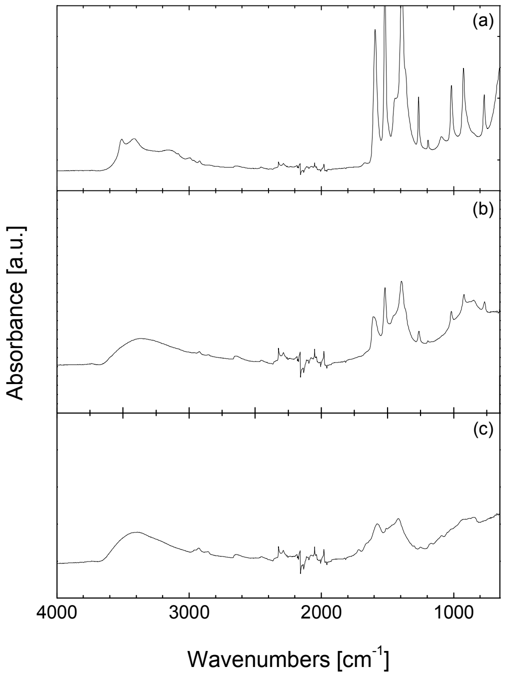

Fig. 7. FTIR spectra of samples with spin-coated Zn(acac)$_2$ layers on glass after various heat treatments: **(a)** as spin coated, **(b)** annealed at 120 °C for 30 s and **(c)** annealed at 200 °C for 20 s.

In order to confirm the order of magnitude of the rate of the reaction, a Zn(acac)$_2$ coated gold slide was brought into contact with the Golden Gate ATR crystal heated at 120 °C. Similarly to Figure 7a, the first spectrum taken before annealing of the layer was characteristic of Zn(acac)$_2$, see **Figure 8a**. It can be seen that a large part of the conversion reaction occurred during the first seconds of heating (**Figures 8b and 8c**).

Furthermore, it was observed that the Zn(acac)$_2$ thermal decomposition was not complete while carried out at 120 °C, even after protracted heating (e.g. up to 4 hours). Although XRD measurements evidenced that part of the precursor was effectively converted into crystalline ZnO, these FTIR measurements suggest that the ETL obtained after Zn(acac)$_2$ decomposition at low temperature most probably consists of a mixture of small ZnO crystals coexisting with another compound. A likely candidate for this residual compound might be hydrozincite, or $Zn_5(CO_3)_2(OH)_6$, based on the spectral match with the experimental results and the fact that it is a common secondary mineral of ZnO.[18]

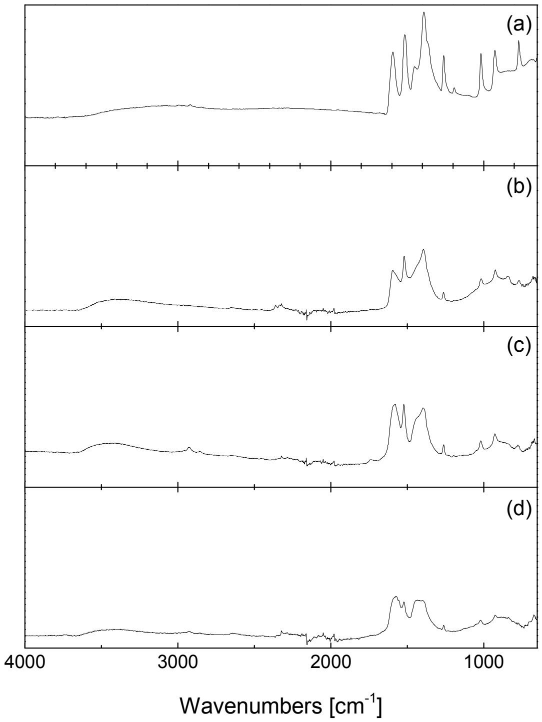

Fig 8. FTIR spectra of samples with spin-coated Zn(acac)$_2$ layers on glass annealed at 120 °C for: **(a)** 0 s, **(b)** 1.2 s, **(c)** 4.8 s, and **(d)** 300 s.

Performance of inverted solar cells with ZnO transport layer

An important finding is that at an annealing temperature of 120 °C the precursor is not completely converted. The resulting ZnO thin film consists of a mixture of small ZnO crystals with hydrozincite residu. Annealing at 200 °C gives nearly complete conversion of Zn(acac)$_2$. However, a temperature of 200 °C is incompatible with R2R processing on PET or PEN substrates where preferably temperatures not higher than 130 °C are used. The question is whether a complete conversion of the precusors is required for optimal solar cell performance. For this purpose we prepared inverted cells with smooth (preheated substrate) and rough Zn(acac)$_2$ layers. As annealing temperature for the Zn(acac)$_2$, 120 °C was chosen. The active layer consisted of P3HT:PCBM in a 1:0.8 weight ratio. The results of the *EQE* and *J-V* measurements are shown in **Figures 9a and 9b**, respectively. It is immediately obvious from the comparison of the *J-V* characteristics that the fill factor of the solar cell with the smooth ZnO layer is much higher than the solar cell with the rough ZnO layer (for which the Zn(acac)$_2$ solution was spin coated on a non-heated substrate). This can be attributed to direct contact between the ITO substrate and the organic materials. The higher work function of ITO as compared to ZnO causes a misaligned electron extraction contact in the regions of direct contact, resulting in a lowered fill factor. This simultaneously explains the magnitude of the measured dark current, as shown in the inset of **Figure 9b**. Hole current can directly flow between the MoO$_3$ contact and the exposed ITO contact, resulting in an increase in the diode dark current. Furthermore the short-circuit current density is largely unaltered, exhibited as well by the quantum efficiency measurements depicted in **Figure 9a**. The subtle spectral differences could be explained by a difference in light scattering between the two ZnO layer structures.

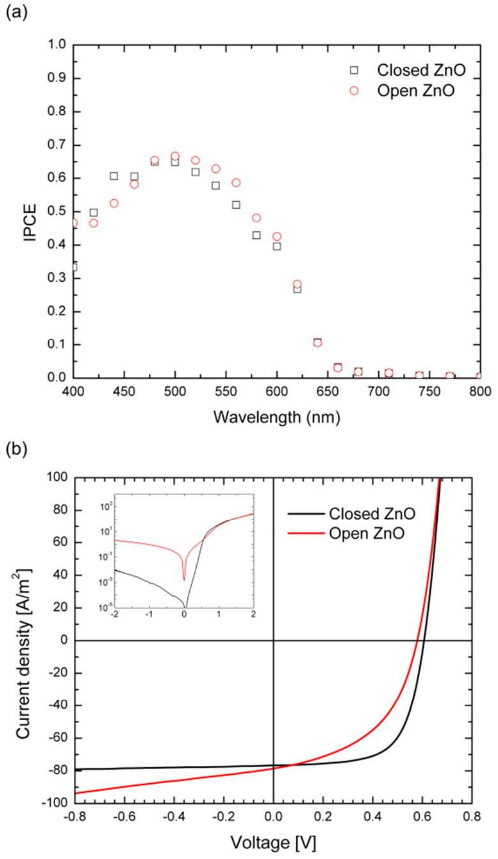

Fig 9. *EQE* and **b.** *J-V* measurement results for inverted cells (ITO/ZnO/P3HT:PCBM/MoO$_3$/Au) prepared with smooth and rough ZnO layers.

In agreement with what has previously been reported by de Bruyn et al.,[7] the equal performance of normal and inverted devices prepared in the same way, and using the Zn(acac)$_2$ precursor annealed at 120 °C, as shown in **Figure 10**, clearly demonstrates that a full conversion of the precursor is not required for solar cell performance. Standard cells with two Ohmic contacts have their V_{oc} determined by the HOMO and LUMO of the donor and acceptor, respectively. [19] If the contact would not have been Ohmic while using the partly crystalline ZnO layer, the V_{oc} of the inverted cell would have been lower than the one of the corresponding direct cell prepared with LiF/Al as Ohmic cathode. The fact that both the inverted cell and direct cell display the same V_{oc} points out that the work function of the partially crystalline ZnO-based layer is suitable for use as low work function cathode. Additionally, it is worth noting that since the work function of the partly crystalline ZnO layer prepared in the present article is similar to the one of crystalline ZnO (4.1 eV [7] vs. 4.2 eV [20]), both types of materials are expected to perform as well as crystalline ZnO that would be obtained after full conversion of the precursor.

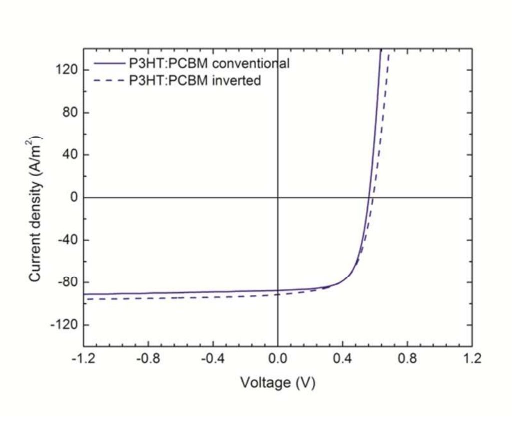

Fig. 10. *J-V* measurement results for an inverted cell prepared with a smooth ZnO layers (ITO/ZnO/P3HT:PCBM/MoO_3/Au) and a direct cell (ITO/PEDOT:PSS/P3HT:PCBM/LiF/Al).

Conclusions

We have demonstrated that prolonged heating times and/or high annealing temperatures are not required to trigger the formation of ZnO from the $Zn(acac)_2$ precursor in order to produce well-performing cells. Though it does not lead to complete conversion of $Zn(acac)_2$ to ZnO, a short 20-s annealing at 120 °C is sufficient. In this respect, this indicates that pure ZnO ETLs are not required since partly crystalline ZnO-based layers are expected to perform as well as crystalline ZnO layers obtained after full conversion of the precursor (i.e. annealing at 200°C). Most important for solar cell performance are the conditions in which the $Zn(acac)_2$ solution is deposited in order to get a closed, smooth ZnO layer.

Acknowledgements

This work was done in the framework of Holst Centre's shared research programs. The work of PdB was supported by the Dutch Polymer Institute (DPI), project DPI# 660. NG and DM thank the HiFlex, geZONd and OzoFab projects for financial support. We gratefully acknowledge Jasper Michels for fruitful discussions and Emile Verstegen, Carry Hermans, Peter Graat, René Bakker, Ruud Soers, Carlo Manders and Toon de Win for technical assistance.

Notes and references

[a] Holst Centre/TNO – High Tech Campus 31 – 5656 AE Eindhoven – The Netherlands

[b] Zernike Institute for Advanced Materials University of Groningen – Nijenborgh 4 – 9747 AG Groningen – The Netherlands

[c] Dutch Polymer Institute – 5600 KN Eindhoven – The Netherlands

[d] Max Planck Institute for Polymer Research - Ackermannweg 10 - 55128 Mainz – Germany

[e] King Abdulaziz University - Abdullah Sulayman - 22254 Jeddah - Saudi Arabia

*Current: SABIC Innovative Plastics - Plasticslaan 1 - PO Box 117 - 4600 AC Bergen op Zoom - The Netherlands

Corresponding authors: Nadia Grossiord Tel: +31 (0)164293441 e-mail address: nadia.grossiord@sabic-ip.com/

1 G. Dennler and S. N. Sariciftci, *Proc. IEEE,* 2005, **93**, 1429.

2 T. D. Nielsen, C. Cruickhank, S. Foged, J. Thorsen and F. C. Krebs, *Sol. En. Mat. Sol. Cells,* 2010, **94**, 1553.

3 H. Hoppe and S. N. Sariciftci, *J. Mater. Res.,* 2004, **19**, 1924.

4 C. Deibel and V. Dyakonov, *Rep. Prog. Phys.,* 2010, **73**, 096401.

5 C. J. Brabec, S. Gowrisanker, J. J. M. Halls, D. Laird, S. Jia and S. P. Williams, *Adv. Mater.,* 2010, **22**, 3839

6 F. C. Krebs, Y. Thomann, R. Thomann and J. W. Andreasen, *Nanotechnology,* 2008, **19**, 424013.

7 P. de Bruyn, D. J. D. Moet and P. W. M. Blom, *Org. Electron.,* 2010, **11**, 1419.

8 N. Grossiord, J. M. Kroon, R. Andriessen and P. W. M. Blom, *Org. Electron.,* 2012, **13**, 432.

9 J. Gilot, I. Barbu, M. M. Wienk and R. A. J. Janssen, *Appl. Phys. Lett.,* 2007, **90**, 1435.

10 D. J. D. Moet, P. de Bruyn, J. D. Kotlarski and P. W. M. Blom, *Org. Electron.,* 2010, **11**, 1821.

11 F. C. Krebs, *Sol. En. Mater. Sol. Cells,* 2009, **93**, 465.

12 S. T. Meyers, J. T. Anderson, C. M. Hung, J. Thompson, J. F. Wager and D. A. Keszler, *J. Am. Chem. Soc.,* 2008, **130**, 17603.

13 R. C. Hoffmann, S. Dilfer, A. Issanin and J. J. Schneider, *Phys. Status Solidi A,* 2010, **207**, 1590.

14 G. Rudolph and M. C. Henry, *Inorg. Chem.*, 1964, **3**, 1317.

15 S. Musić, A. Šarić and S. Popović, *Ceram. Int.,* 2010, **36**, 1117.

16 T. Arii and A. Kishi, *J. Therm. Anal. Cal.,* 2006, **83**, 253.

17 U. Seetawan, S. Jugsujinda, T. Seetawan, C. Euvananont, C. Junin, C. Thanachayanont, P. Chainaronk and V. Amornkitbamrung, *Solid State Sc.,* 2011, **13**, 1599.

18 W. Preis and H. Gamsjäger, *J. Chem. Thermodynamics,* 2001, **33**, 803.

19 V. D. Mihailetchi, P. W. M. Blom, J. C. Hummelen and M. T. Rispens, *J. Appl. Phys.*, 2003, **94**, 6849.

20 S. Gutman, M. Conrad, M. A. Wolak, M. M. Beerbom and R. Schlaf, *J. Appl. Phys.,* 2012, **111**, 123710.

TABLE OF CONTENTS

Manuscript ID TC-ART-06-2014-001393

Partly crystalline ZnO-based transport layers made from precursor solutions are characterized and used to produce well-performing inverted organic solar cells.